Doctoral School of Humanoid Technologies

University of Genova - Genova, January 23, 2006

Part 1:Kinestetic-like sensing for gesture and posture recognition and classification

Part 2: Polymer based biomimetic actuators as artificial muscle

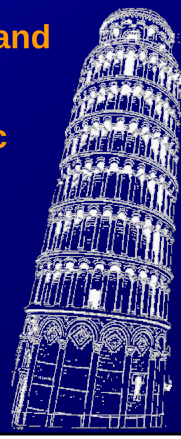

Prof. Danilo De Rossi

University of Pisa

Interdepartmental Research Centre "E. Piaggio"

Part 1

Monitoring body kinematics, posture and gesture

- Rehabilitation
- Sport
- Multimedia

Sensing Garments

- What is presented here are garments able to detect posture and movements.
- Piezoresistive sensors are integrated in the fabric.

- **Portable**
- **Unobtrusive**

Wearable sensors - Static characterization

- Carbon inclusions in the rubber make it conductive. The value of resistance changes (with repeatability) if the specimen is stretched.
- Gauge Factor (GF), Temperature Coefficient of Resistance (TCR) and R_0 of a specimen depend on its **shape** and change with the **percentage** of the components and of the solvent (trichloroethylene)

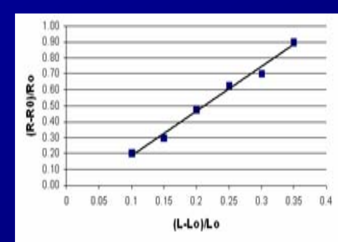

- Galley proofs 5 mm (width).
- Resistance (unstretched): 1 KOhm per cm.
- GF:2.8 (before saturation that occurs for displacement greater than 40%).
- TCR : 0.08°K^{-1}.

Wearable sensors - Dynamical characterization(1)

Dynamical properties show some peculiarities:

- Sensor fabric solicited by a step in length ⇒ its resistance **increases** up to a maximum value, then it **decreases** to a regime value.
- **Transient time is too long** to allow raw data to code for human movements.
- After a decreasing step in length, the resistance value **increases** again for a while, then it **decreases**.

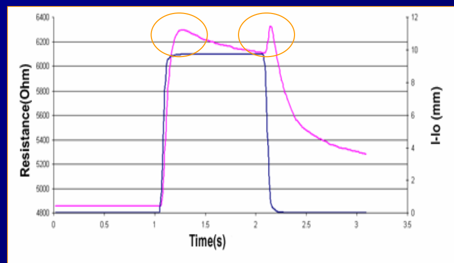

Wearable sensors - Dynamical characterization(2)

Specimens have been tested by trapezoidal inputs:

- Slope of the inputs kept fixed ⇒ heights of the peaks and transient time remain the same.

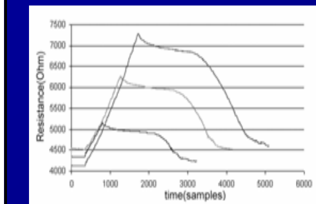

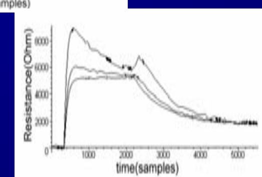

- By increasing the velocity of the extension, height of the peaks increases.
- Since peaks are always greater than their final value

  ⇒ a non-linear pre-elaboration of the inputs is necessary.

Wearable sensors - Dynamical characterization(3)

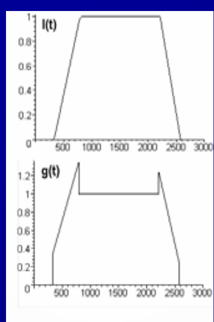

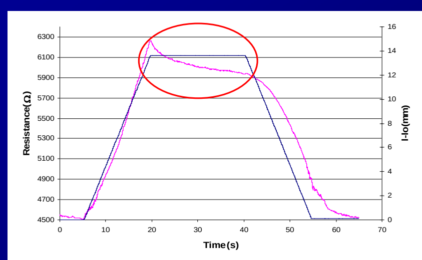

Let's: $g(t) = a_1 l(t) + a_2 \dot{l}(t) + a_3 \left(\dot{l}(t)\right)^2$

Sensor behavior characterization →
$$\begin{cases} \dot{g}(t) = 0 \\ \dot{g}(t) \neq 0 \end{cases}$$

The transient time $(\dot{g}(t) = 0)$

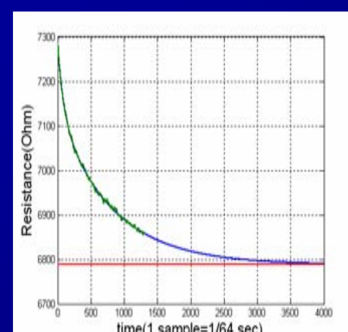

- two-pole regression on decreasing step (of g(t)) after a trapezoidal input (in l(t))
- The two pole values remain the same for different extensions and slopes
- The coefficient C_0 coincides with the regime value

$$R(t) = C_0 + C_1 e^{-\omega_1 t} + C_2 e^{-\omega_2 t}$$

- A regression with a larger number of poles does not give any further advantage.

During the length change ($\dot{g}(t) \neq 0$)

The system $g(t) \xrightarrow{sensor} R(t)$ has been linearized:

$$\begin{bmatrix} \dot{R}(t) \\ R(t) \end{bmatrix} = e^{A(t-t_0)} \begin{bmatrix} \dot{R}(0) \\ R(0) \end{bmatrix} + \int_{t_0}^{t} e^{A(t-\tau)} \begin{bmatrix} 0 \\ g(\tau) \end{bmatrix} d\tau$$

Where:

$$g(t) = a_1 l(t) + a_2 \dot{l}(t) + a_3 \left(\dot{l}(t)\right)^2 \qquad A = \begin{bmatrix} 0 & 1 \\ -\omega_1\omega_2 & -(\omega_1+\omega_2) \end{bmatrix}$$

- By using a linear regression on experimental data obtained in our laboratory, a_1, a_2, a_3 have been determined.
- The heights of the peaks uniquely determine the values of the three coefficients.

Test of the model

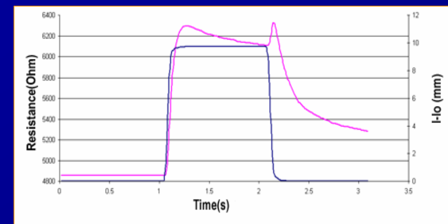

Solicitation and actual response

Model response

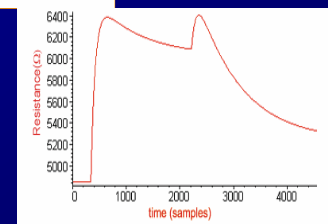

The reconstruction of the length

$$\begin{bmatrix} \ddot{R}(t) \\ \dot{R}(t) \end{bmatrix} = A \begin{bmatrix} \dot{R}(t) \\ R(t) \end{bmatrix} + \begin{bmatrix} 0 \\ g(t) \end{bmatrix} \Rightarrow g(t) = \left(\begin{bmatrix} \ddot{R}(t) \\ \dot{R}(t) \end{bmatrix} - A \begin{bmatrix} \dot{R}(t) \\ R(t) \end{bmatrix} \right)_2$$

l(t) is the solution of the Cauchy's problem:

$$\begin{cases} a_1 l(t) + a_2 \dot{l}(t) + a_3 \dot{l}(t)^2 = g(t) \\ l(0) = l_0 \\ \dot{l}(0) = \dot{l}_0 \end{cases}$$

- Unfortunately, the noise which affects data partially invalidates the numerical derivation.
- This procedure can be used off-line.
- To use this procedure on-line, a wide filtering is necessary (with delay)
- Noise reduction is under study

Length reconstruction: a fast algorithm

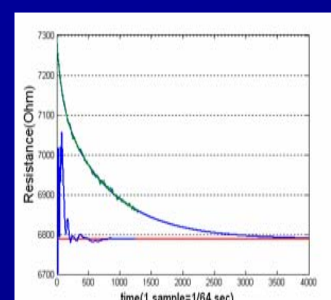

- The model obtained can be employed to realize an effective length detection
- a first exponential regression (after a step in l(t)) to evaluate the poles $\omega_i (= \omega_i^0)$ is necessary.
- The ω_i value is continuously calculated using the newly available samples

$$\omega_i = \omega_i^0 \Rightarrow \dot{l}(t) = 0$$

- By computing at each time the regime value, the length of the sensors is determined when the system is motionless.
- The algorithm reduces the transient time of about <u>95%</u>. The first inaccuracy is due to the noise of the system.

The sensing glove - Electrical topology

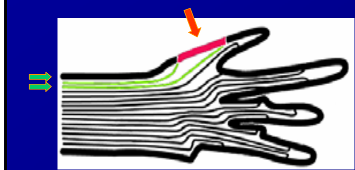

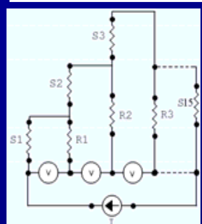

S_i: sensors

R_i: wires

- The bold black track represents the set of sensors (connected in series)
- The most important joints of the hand are covered.
- The thin tracks represent the connection between sensors and the acquisition system.
- Connection wires too show piezoresistive properties.
- By using a high-impedance-input acquisition system, wire resistance (and its variation) is neglected.

The glove as posture recorder

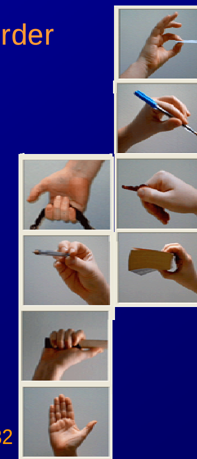

- When the hand holds a certain position ⇒ the sensors assume corresponding values.
- if the number of sensors is large enough ⇒uniqueness of position represented by sensor values.
- good capabilities of repeatability, even if it is removed from the hand and re-worn (by the same subject).
- **Posture and movements can be recorded and distinguished.**
- In particular, we have tested this capability on 32 different functionally relevant postures: the basic grips and the signs of the American sign language

The glove as posture detector

- The system hand+glove have to be identified.
- A set of basic position are recorded – the following discrete map:

$$F^*: \Re^n \supset L \supset \theta \mapsto (s_1, s_2, \ldots, s_n) \in \Sigma \subset \Re^m$$

n = degree of freedom
m = number of sensors

is defined.

- Each component of F^* *is* Piecewise Linear- interpolated on $\Re^n$
- Multivariate interpolation has been executed by realizing an algorithm which share the hypercubes into hypertetrahedra. A minimal partitioning has been found.

$$f_i: \Re^n \supset \Theta \ni (\theta_1, \theta_2, \ldots, \theta_n) \mapsto s_i \subset S_i^* \in \Re$$

The glove as posture detector - Inversion

- The pseudo-inverse $F^{\dagger}$ of the interpolated F is used to define a Newton-Raphson iterative process.

$$\begin{cases} \theta_{k+1} = \theta_k + F^{+}(s_k - s_{read}) \\ \theta_0 \quad any \end{cases}$$

- Example: Posture reconstruction for the forefinger

McPh	IPprox	IPdist
45	22.5	18.5
45.6489	25.3125	15.468

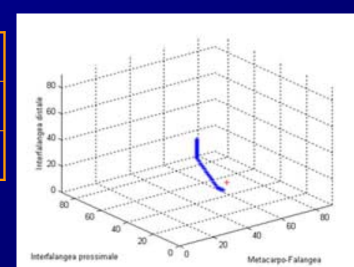

- **Error: less then 4%**

The Upper Limb Kinesthetic Garment

An upper limb kinesthetic garment (ULKG) which detect the posture of wrist, elbow and shoulder has been developed by using the same technology and it is going to be used in post-stroke patients rehabilitation (My-Heart, EU-IST, VI framework).

The ULKG is integrated in a health care service which allow patients to continue the rehabilitation training at home or in unsurveyed environments, and without the help of physicians, after the intensive rehabilitation period.

The Upper Limb Kinesthetic Garment

The ULKG acquire information on the joints of the upper limb by 20 sensors spread on a shirt. It monitors the shoulder, elbow and wrist joints. (7 DOFs).

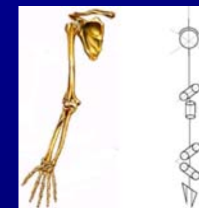

The same technology used to realize the glove avoids the employment of metallic wires. All the movements result unbounded.

Although the ULKG is mainly used to discriminate movements previously recorded (as sequences of position), it needs an identification (based on a comparison with electrogoniometer output) to represent these movements in term of joint angles and permit a graphical feedback.

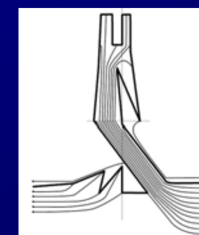

The Upper Limb Kinesthetic Garment

In this way, the garment is capable to drive a virtual (3D) pointer which let the patients to execute trail programs and have a performance evaluation.

An avatar included in the service shows to the patient the exercise he has to perform, which is coded by a path in the 7 DOFs upper limb workspaces.

The rehabilitation protocol, composed by series of exercises, is settled by rehabilitators and it compounds movements devoted to the recover of reaching and grasping functionalities. It can be remotely modified and improved by therapists.

The Upper Limb Kinesthetic Garment

Results from trials on the ULKG: the device output (blue paths) is compared with the results of a motion detection executed by commercial electrogoniometers (red paths).

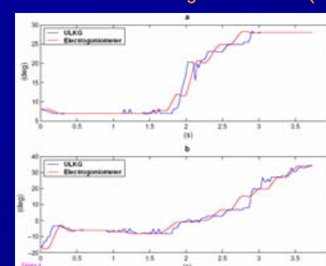

Extension (a) and flexion (b) angles versus time of the shoulder

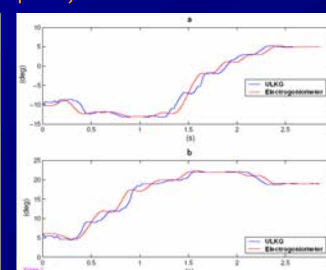

Flexion (a) and abduction (b) angles of the wrist versus time

The Upper Limb Kinesthetic Garment

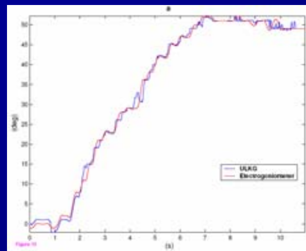

Flexion angle of the elbow vs time

Acquisition of joint angle values for 15 hand DOFs

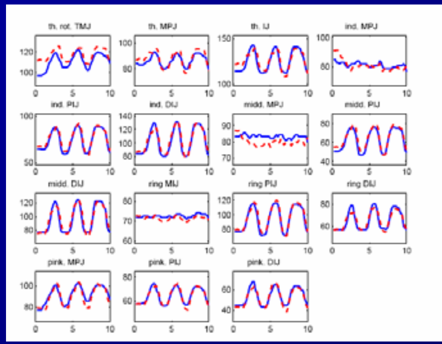

The dashed lines are the CE sensing glove outputs while the continuous lines are cyberglove outputs

Part 2
EAP Actuators

CLASSIFICATION OF ELECTROACTIVE POLYMERS

Mechanism of activation	Materials
Mass/ion transport (ionic EAPs)	Conducting polymers Polyelectrolyte gels Ionic polymer-metal composites Carbon nanotubes
Electric field (electronic EAPs)	Dielectric elastomers Piezoelectric polymers Electrostrictive polymers Liquid crystal elastomers

Actuator Type (specific example)	Maximum Strain (%)	Maximum Pressure (MPa)	Specific Elastic Energy Density (J/g)	Maximum Efficiency (%)	Relative Speed (full cycle)
Dielectric Elastomer					
(Acrylic)	380	7.2	3.4	60–80	Medium
(Silicone)	63	3.0	0.75	90	Fast
Electrostrictive Polymer (P(VDF-TrFE)	4.3	43	0.49	~80 est.	Fast
Carbon Nanotube	> 2.5	> 1.0	> 0.013	< 10?	Medium
Liquid Crystal Elastomer	> 35	> 0.3	> 0.10	< 10?	Slow
Responsive Gels (Polyelectrolyte)	> 40	0.3	0.06	30	Slow
IPMC (Nafion)	10	1.0	0.025	< 10?	Medium
Conducting Polymer (Polypyrrole)	15	20	3	< 10?	Slow
Natural Muscle					
Peaks in nature	100	0.80	0.04	-	Slow-Fast
Human Skeletal	> 40	0.35	0.07	-	Medium

EAP Actuators

Polyelectrolyte Gels

polymer gel:
elastic cross-linked polymer network filled with a fluid

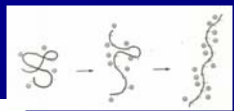

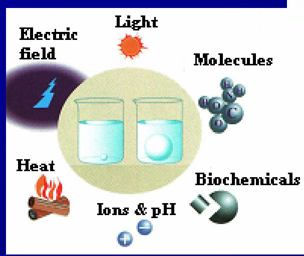

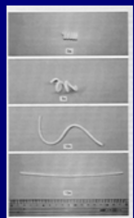

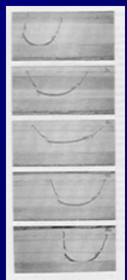

EAP Actuators

Ion Polymer-Metal Composites (IPMC)

polymeric membrane containing ionic liquids,
covered by metal electrodes.
A low electric field induces electrophoretic migration of ions,
causing bending of the membrane.

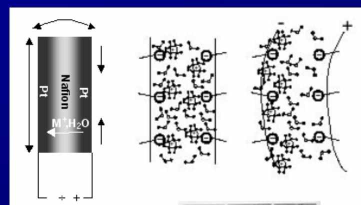

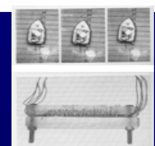

(from M. Shahinpoor, Y. Bar-Cohen et al.)

EAP Actuators

Conducting polymers (CP)

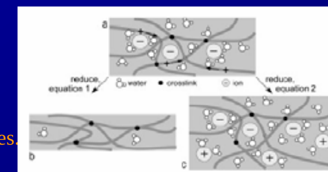

Electrochemical cell with CP electrodes.

A low voltage applied between the electrodes causes deformations of the active material, due to Faradic exchange of ions with the electrolyte

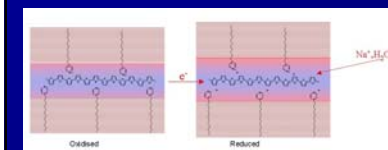

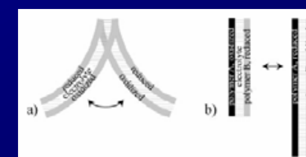

EAP Actuators

Conducting polymers (CP)

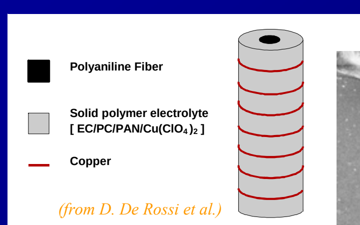

(from D. De Rossi et al.)

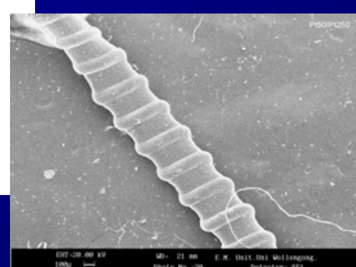

(from G. Spinks, G. Wallace et al.)

EAP Actuators

Conducting polymers (CP)

Polypyrrole–metal coil composite actuators
(from Hara,Zama,Takashima and Kaneto)

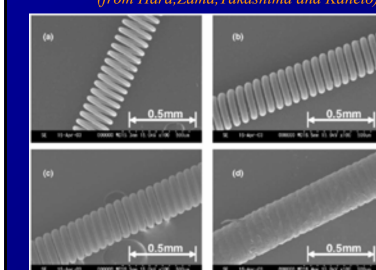

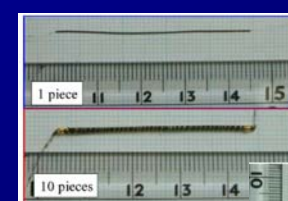

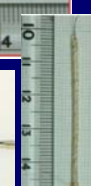

EAP Actuators

Conducting polymers (CP)

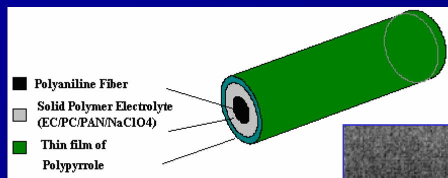

(from D. De Rossi et al.)

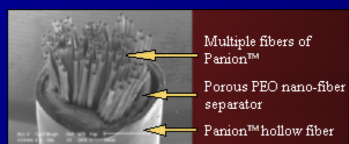

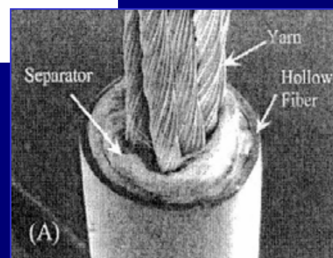

(from B. Mattes et al.)

EAP Actuators

Carbon NanoTubes (CNT)

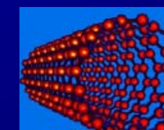

Electrochemical cell with CNT electrodes.

A low voltage applied between the electrodes causes deformations of the active material, due to a variation of the double-layer charge around nanotubes

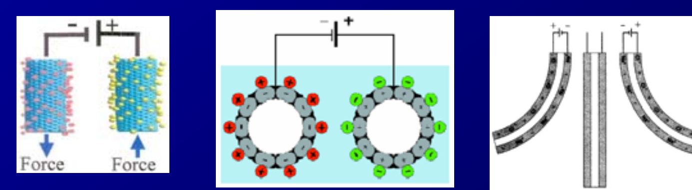

(from R. Baughman et al.)

EAP Actuators

Carbon NanoTubes (CNT)

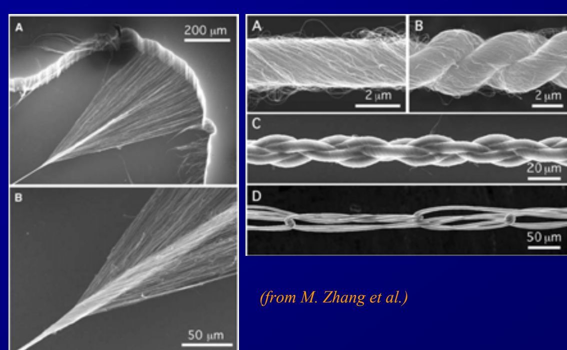

(from M. Zhang et al.)

EAP Actuators

Electrostrictive Polymers

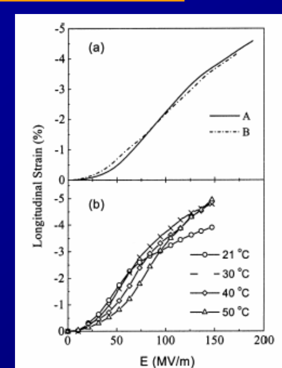

Strain = Q E²

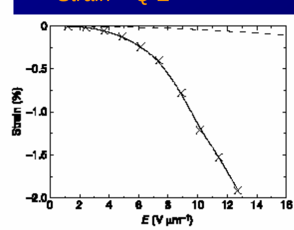

EAP Actuators

Liquid crystalline elastomers

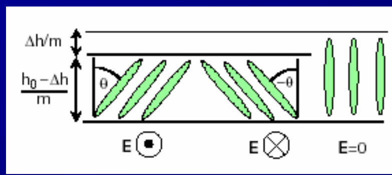

(from W. Lehmann et al.)

EAP Actuators

Dielectric Elastomers (DE)

Thin elastomeric film sandwiched between two compliant electrodes.

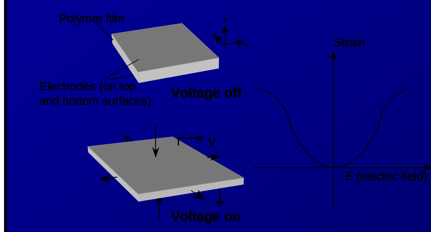

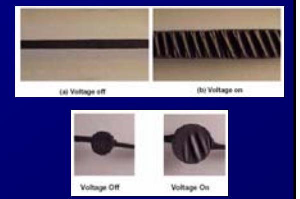

(from R. Pelrine, R. Kornbluh et al.)

Electrostatic pressure:

$$p = \varepsilon_0 \varepsilon_r E^2$$

ε_0 = free – space dielectric permittivity
ε_r = polymer dielectric constant
E = applied electric field

Genova, January 23, 2006

EAP Actuators

Dielectric Elastomers (DE)

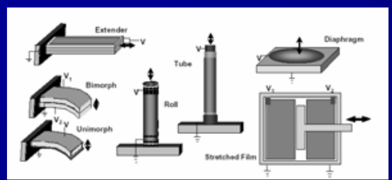

(from R. Pelrine et al.)

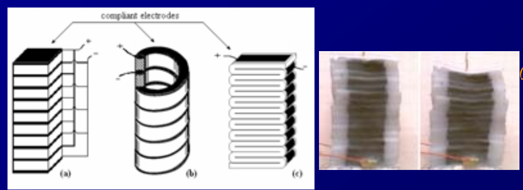

(from Carpi et al.)

Genova, January 23, 2006

Dielectric Elastomer Actuators

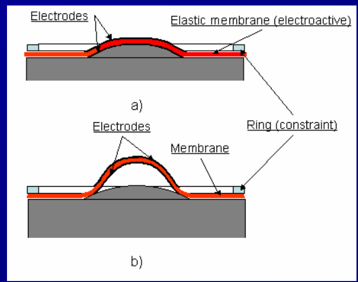

Genova, January 23, 2006

Dielectric Elastomer Actuators

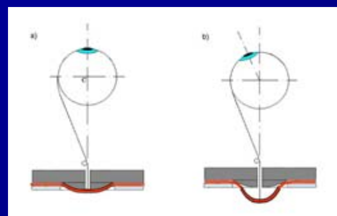

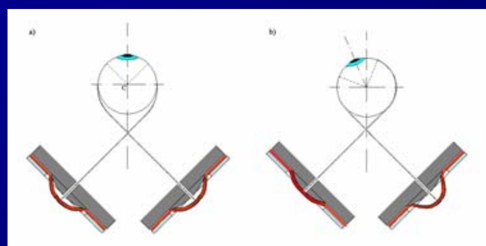

Genova, January 23, 2006

Dielectric Elastomer Actuators

Genova, January 23, 2006

Dielectric Elastomer Actuators

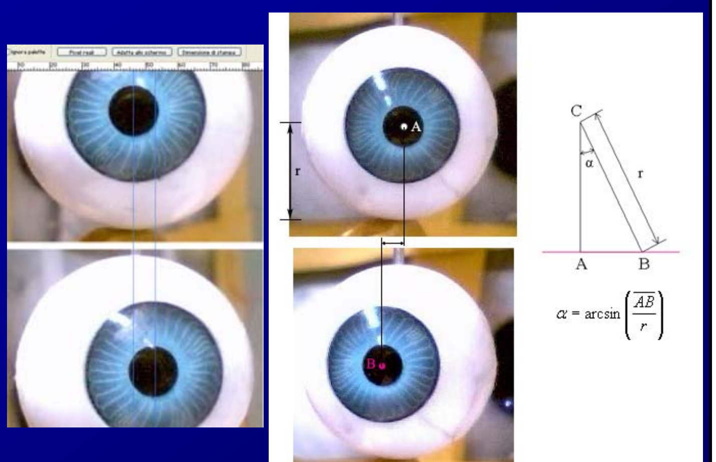

Genova, January 23, 2006

Dielectric Elastomer Actuators

Agonist-antagonist couple of rectus-type muscles

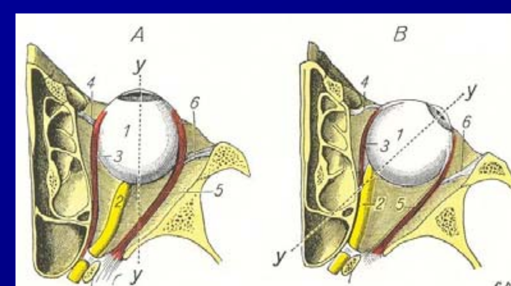

Genova, January 23, 2006

Dielectric Elastomer Actuators

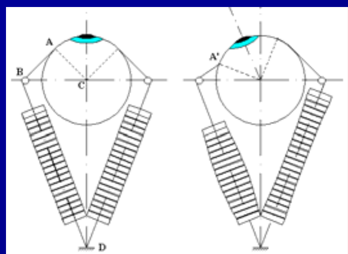

1st configuration:

2nd configuration:

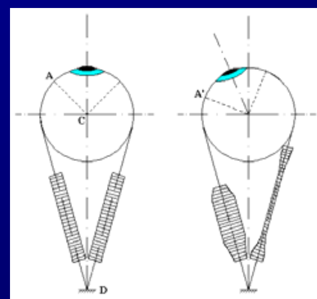

Dielectric Elastomer Actuators

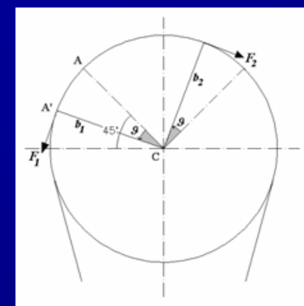

$$F_1 = F_2$$

$$F_1 = F_{a1} + F_{p1}$$

$$F_{p1} = Y_1 Vol_1 \left(\frac{1}{l_{01}} - \frac{1}{l_1} \right)$$

$$F_{a1} = pA_1$$

$$p = \varepsilon_0 \varepsilon_r E^2$$

$$F_2 = Y_2 Vol_2 \left(\frac{1}{l_{02}} - \frac{1}{l_2} \right)$$

$$p \frac{1}{l_{1(\vartheta)}} + Y \left(\frac{1}{l_0} - \frac{1}{l_{1(\vartheta)}} \right) = Y \left(\frac{1}{l_0} - \frac{1}{l_{2(\vartheta)}} \right)$$

Dielectric Elastomer Actuators

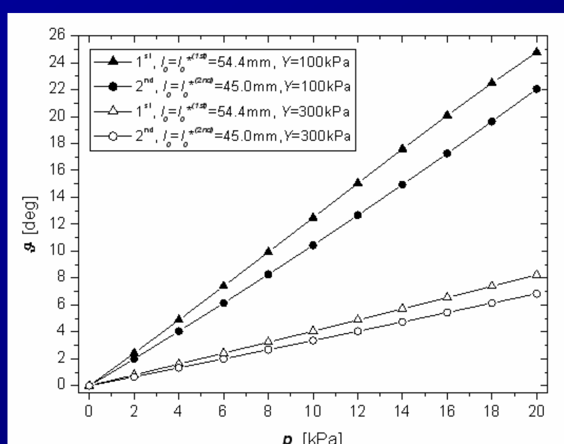

Dielectric Elastomer Actuators

Feasibility study for the actuation of an anthropomorphic skeleton of an upper limb

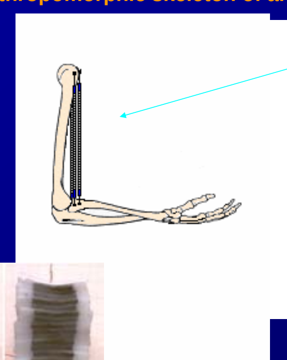

Bundle of 4 actuators

Dielectric Elastomer Actuators

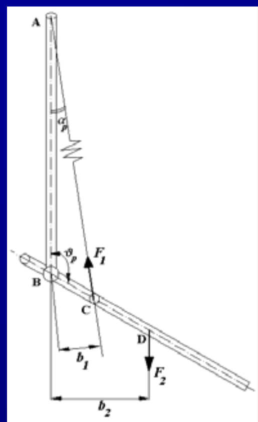

$$F_1 b_1 = F_2 b_2$$

$$F_l = 4(F_p + F_e)$$

$$F_p = Y\,Vol\left(\frac{1}{l_0} - \frac{1}{l}\right)$$

$$F_e = pA$$

$$p = \varepsilon_0 \varepsilon_r E^2$$

Dielectric Elastomer Actuators

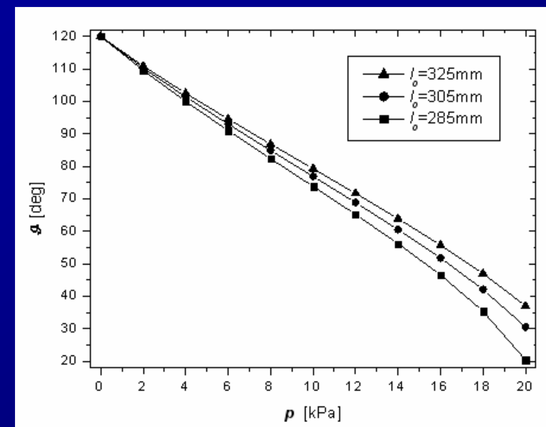

Dielectric Elastomer Actuators

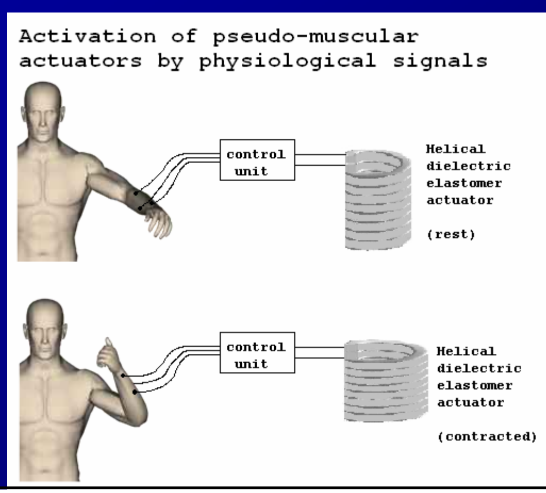

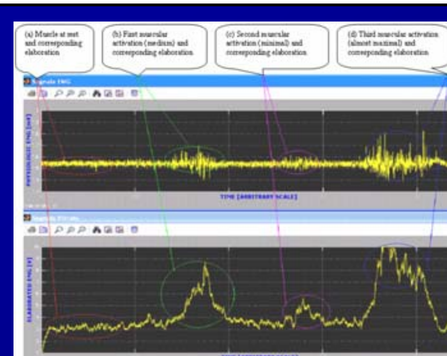

EMG activation

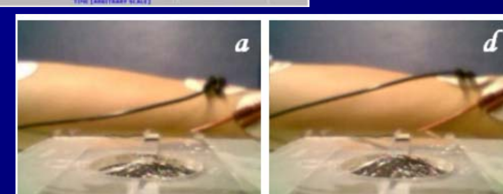

Acknowledgements

The support of

EU Commission through IST 507816 research Project *MyHeart*

DARPA and ONR-IFO through NICOP grant N00014-01-1-0280, Pr N 01PR04487-00

Contract ESA- Kayser n°18548/04/NL/PA

EU Commission through (NMP2- CT-2004-505864) *Flexifunbar Project*

is gratefully acknowledged